Dyes and Pigments 139 (2017) 587–592

Contents lists available at ScienceDirect

Dyes and Pigments

journal homepage: www.elsevier.com/locate/dyepig

A NIR turn-on fluorescent probe applied in cytochrome P450 reductase detection and hypoxia imaging in tumor cells

Lei Cui [a, *], Yanping Shi [a], Shuping Zhang [a], Luliang Yan [a], Huan Zhang [a], Zhenran Tian [a], Yingying Gu [a], Ting Guo [c, **], Junhai Huang [b, ***]

[a] College of Science, University of Shanghai for Science and Technology, Shanghai 200093, China
[b] Zhangjiang Institute, China State Institute of Pharmaceutical Industry, 1599 Zhangheng Road, Shanghai 201203, China
[c] College of Pharmaceutical Sciences and Chinese Medicine, Southwest University, Chongqing 400715, China

ARTICLE INFO

Article history:
Received 7 December 2016
Received in revised form
23 December 2016
Accepted 25 December 2016
Available online 28 December 2016

ABSTRACT

In vivo monitoring of the hypoxic area is urgently required. Near infrared (NIR) fluorescence-active fluorophores with excellent photo stability are preferable for *in vivo* imaging. A novel rational designed turn-on fluorescent probe with high selectivity and long-wavelength was synthesized which was applied in bioreductase (cytochrome P450 reductase which overexpressed in tumor cells) and hypoxia detection. The NIR probe (**AZO-DCM**) is based on a photo stability fluorophore dicyanomethylene-4*H*-pyran dye (**DCM**) with an azo bond as probe quencher and hypoxic trigger. After reacted with cytochrome P450 reductase, azo bond was cleaved and **DCM** released with fluorescent on. The designed probe showed high anti-interference ability which cannot disturb by many interfering substances, such as biothiols, inorganic salts (included sulfite salt) and amino acid. **AZO-DCM** performed good selectivity and sensitivity to cytochrome P450 reductase and hypoxia. The fluorescent intensity was increased more than 150-fold after response to cytochrome P450 reductase and NADH system in 4 min. The reaction mechanism also proved by HPLC experiment. Probe **AZO-DCM** displayed excellent properties in identifying different hypoxic status of tumor cells *in vivo*.

1. Introduction

As an important character of tumors, hypoxia was found in more than 60% solid tumors. The tumor oxygenation status tampers the therapeutic effects of radiotherapy, chemotherapy, biotherapy and thermotherapy [1,2]. Tumor hypoxic cells not only show low sensitivity to radiotherapy, but also resist to chemotherapy and biotherapy [3,4]. Detection of hypoxia is helpful for the establishment of clinical therapeutic plan and the patient-oriented individual therapeutic plan [5]. Lots of researchers had developed many methods to detect hypoxia, such as immunostaining, positron emission tomography (PET), magnetic resonance imaging (MR) and doppler optical coherence tomography [6–9]. With the advantage of high sensitivity, high resolution, adjustable emission wavelength, real-time monitoring and non-invasiveness, fluorescent imaging had received more attention and been widely applied in biological detection [10–14].

Several papers about hypoxia imaging reported mainly focused on nitroreductase (NTR) which can reduce nitro group to amine. Based on this reaction, several papers were published and some got good results [15–19]. Recently, a new chemical group azo bond was found effective to hypoxia and showed good performance under different oxygen partial pressure [20–22]. Nagano group first reported the cyanine dye connected to a commercial available quencher BHQ-3 with an azo group. Through the effect of FRET, the fluorescence can be quenched completely. Probe displayed good performance in detecting acute ischemic and related hypoxia. Here, we designed a new probe which based on dicyanomethylene-4*H*-pyran dye and azo functional group with NIR emission wavelength, which was easier to synthesis and performed higher sensitivity to cytochrome P450 reductase and hypoxia.

* Corresponding author.
** Corresponding author.
*** Corresponding author.
E-mail addresses: cuilei15@usst.edu.cn (L. Cui), guoting15@swu.edu.cn (T. Guo), huangjunhai@sinopharm.com (J. Huang).

http://dx.doi.org/10.1016/j.dyepig.2016.12.062
0143-7208/

2. Experiment section

2.1. Instruments and chemicals

UV–visible absorption spectra were obtained using a UV–visible spectrometer (Scinco 3000 spectrophotometer). Fluorescent spectra were performed on a Hitachi F-7000 luminescence spectrophotometer in 10 × 10 mm quartz cells fluorescence spectrophotometer at 37 °C. ^{1}H and ^{13}C spectra were measured using a Bruker ARX 300 NMR spectrometer. The molecular mass was acquired using ion trap time-of-flight mass spectrometry (MS-TOF). The pH values of buffers were adjusted using a Sartorius PB-10 basic pH meter. Fluorescence imaging experiments were performed on confocal microscope (Olympus, IX81, JPN) at $\lambda_{ex} = 500$ nm. A liquid chromatography system from Agilent Technologies (Agilent, American) was applied to all chromatography tests. Deionized water was used to prepare all aqueous solutions.

2.2. Spectroscopic materials and methods

Double distilled water was used to prepare all aqueous solutions. All spectroscopic measurements were performed in PBS buffer (30% DMSO and 0.1% Tween 80) except cytochrome P450 reductase assay in 0.1 M phosphate buffer (pH 7.4, 10% DMSO and 0.3% Tween 80) at 37 °C. All pH measurements were made with a Sartorius basic pH-Meter PB-10. Samples for absorption and fluorescence measurements were contained in 1 cm × 1 cm quartz cuvettes (100 μL volume).

2.3. Cytochrome P450 reductase assay

Cytochrome P450 Reductase (Rabbit liver, purchased from Sigma-Aldrich) experiments were performed in 1 cm × 1 cm quartz cuvettes. Stock solutions of probe **AZO-DCM** were prepared in pure DMSO (0.1 mM). Experimental system is PBS buffer (0.1 mM, pH = 7.4) in 37 °C water bath. The concentration of **AZO-DCM** in solution is 1 μM. The dosage of Cytochrome P450 reductase is 1U/mL and NADPH is 1 mM. Argon gas was bubbled into the **AZO-DCM** solution for one hour to create the hypoxic environment. The emission intensity was collected from 540 nm to 700 nm with excitation at 500 nm.

2.4. HPLC for probe ***AZO-DCM*** with cytochrome P450 reductase

HPLC was performed on a ZoRBAX RX-C18 column (Analytical 4.6 × 250 mm 5 μm, Agilent) with a HP 1100 system. The HPLC solvents employed were 15% acetonitrile and 85% methanol. The HPLC conditions were as follows: solvent A: solvent B = 0:100 (0 min)–100:0 (20 min), flow rate 1.2 mL/min, detection by UV/Vis (254 nm and 500 nm). The reaction solution of **AZO-DCM** (10 μM), NADPH (1 mM) and cytochrome P450 reductase (1 U/mL) was incubated in PBS buffer (0.01 M PBS, pH = 7.4, contains 1% DMSO, 0.1% Tween 80) for 3, 5, 10, 15 and 30 min. When time is up, the solution was filtered through filter to remove reductase. After nitrogen purged and dried for 1.5 h, the crude product was analyzed by HPLC.

2.5. Cell culture and imaging

HeLa and A549 cells were obtained from American Type Culture collection and were grown in RPMI-1640 (Hyclone), supplemented with 10% FBS (Gibco), 2 mM L-Glutamine, 100 U/mL penicillin and 100 μg/mL streptomycin. Cells were incubated in a 5% CO_2 incubator at 37 °C and passaged with sub-cultivation ratio of 1:4 every two days. HeLa cells were seeded in 24-well plates under culture medium. For fluorescence imaging, cells were incubated under normoxic (21% pO_2) and hypoxic (10%, 5%, 1% pO_2) conditions for 6 h at 37 °C. Then the cells were washed with PBS buffer (pH 7.4) and were treated with 1 μM **AZO-DCM** in FBS-free RPMI-1640 for 30 min. HeLa cells were washed three times with PBS buffer before taken images which were performed with Nikon (Eclipse Ti-E 2000). The fluorescent field was collected with 500 ms exposure time using a Texas Red filter and with 500 ms exposure time for bright field.

3. Results and discussion

3.1. Synthesis and structural characterization

Probe **AZO-DCM** was synthesized according to previous methods [23,24], as shown in Scheme S1. The intermediate and products were confirmed by ^{1}H NMR, ^{13}C NMR and HR-MS. (see Supplementary information).

3.2. Spectrum of probe ***AZO-DCM*** and fluorophore ***DCM***

UV–Vis spectrum and fluorescent emission about probe **AZO-DCM** (10.0 μM) and fluorophore **DCM** (10.0 μM) which dissolved in PBS buffer with 30% DMSO was performed (Fig. 1). Probe **AZO-DCM** with an azo bond showed a longer absorption wavelength at λ_{max} 520 nm and fluorophore **DCM** at λ_{max} 500 nm. For fluorescent spectrum of **AZO-DCM**, the absorbed energy was easy to deplete due to the vibration of azo bond, there was nearly no fluorescent signal. Lots of commercialized compounds contained azo bond, like BHQ-1, BHQ-2 and BHQ-3, were widely used as an effective quencher for cyanine dyes. However, fluorophore **DCM** performed a strong fluorescent at the wavelength of 650 nm. The huge difference between fluorophore **DCM** and probe **AZO-DCM** means azo bond is an excellent potential receptor for hypoxia detection. After the azo bond of probe **AZO-DCM** was reduced to amine, an obvious fluorescent signal could be detected.

3.3. Spectrum of probe and response toward Na_2SO_3

Prof. Cao have reported several researches about azo bond which can be reduced by sulfite [25]. To investigate the selectivity of the probe **AZO-DCM**, the UV–Vis absorption and fluorescence response of the probe to sodium sulfite were tested (Fig. 1). The UV–Vis absorption spectra showed there was a blue shift about 20 nm after treated with sodium sulfite, which means the azo bond was not exist. The maximum absorption wavelength was changed from 520 nm to 500 nm, correspondingly, the color was changed from light purple to orange-red. As shown in Fig. 1b, no fluorescent signal was detected after sodium sulfite added. Possibly, the addition of sulfite to C=C which resulted the ICT structure destroyed. This mechanism had also been applied in design of fluorescent probe for sulfite [26,27]. This experiment showed the most possible interfering substance sulfite was excluded, which did a good foundation for the application in cell.

3.4. Response towards cytochrome P450 reductase

To further examine whether the probe **AZO-DCM** was suitable for the hypoxia detection, cytochrome P450 reductase (1 U/mL) which contain various reductases was applied assay *in vitro*. In order to create a hypoxic environment, argon was bubbled in to **AZO-DCM** solution (3.0 μM, PBS buffer with 10% DMSO, 0.1% Tween 80, pH 7.4) for 15 min, then cytochrome P450 reductase was added. Upon the addition of NADPH (100 μM, as a cofactor of cytochrome P450 reductase), a dramatic fluorescent enhancement was

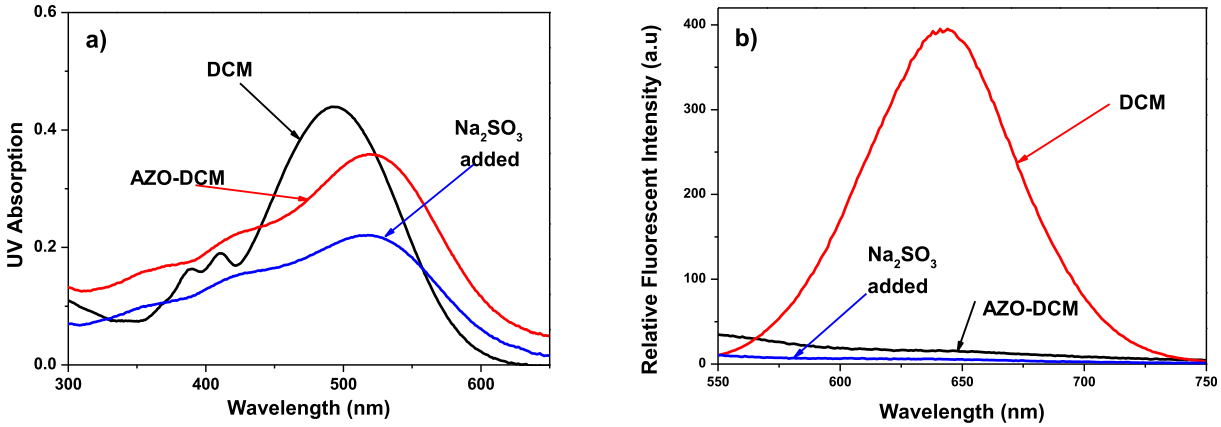

Fig. 1. Absorption (left) and fluorescent emission (right) spectra of **AZO-DCM**, **DCM** and the reaction solution of **AZO-DCM** with sodium sulfite in phosphate buffered saline (0.01 M, pH 7.4) containing 30% DMSO and 0.1% Tween 80 at room temperature.

observed at around 650 nm with excitation at 500 nm. The fluorescent intensity was increased about 156 folds (Fig. 2a) under argon atmosphere (1% pO_2). But there was slight fluorescence change, about 1.5 folds, under normoxia condition (20% pO_2). The fluorescent peak appeared at 650 nm is corresponding to the fluorescent emission of the fluorophore **DCM**, which means the azo bond was reduced and cleaved successfully by the reductase with the release of fluorophore **DCM** under hypoxia condition. As a control, without cytochrome P450 reductase, no fluorescent signal was observed in air (21% pO_2) saturated or argon atmosphere (1% pO_2) solution with cofactor NADPH.

To further understand the catalytic process of cytochrome P450 reductase, the kinetics of **AZO-DCM** in the presence of NADPH was measured under different condition (hypoxia/normoxia). The fluorescence data was recorded at the wavelength of 650 nm (Fig. 2b). Under hypoxia condition, the fluorescence reached a plateau within 5 min. As a contrast, the fluorescence was weak and the change of fluorescent intensity was negligible in the next 20 min under normoxia condition. In this test, it's easier to observe the large S/N value in fluorescent intensity between hypoxia and normoxia. The experiment also guaranteed probe **AZO-DCM** for detection of hypoxia cells.

3.5. Selective response of probe *AZO-DCM*

To further evaluate the application in living cells, some possible interference substances were investigated [28–30]. The probe **AZO-DCM** was treated with reductants (Vc and glutathione), biothiols (cysteine and dithiothreitol), inorganic salts ($FeCl_2$), Glucose, NADPH or amino acid (tyrosine). The concentration of reduced biological reductants is less than 1 mM in normal physiological conditions. As shown in Fig. 3, up to 100 equiv. of interference substances did not induce any noticeable fluorescent signal enhancement. The selectivity was also studied in the present of cytochrome P450 reductase with 100 equiv. of other biological reductants. The changes of fluorescence intensity were also negligible except NADPH. Only the mixture of NADPH, cytochrome P450 reductase and **AZO-DCM** presented strong fluorescent at 650 nm. Therefore, it can be concluded that **AZO-DCM** displayed high selectivity for bioreductase and stable in biological system.

3.6. HPLC analysis of metabolism of *AZO-DCM* reacted with cytochrome P450 reductase

The mechanism of probe **AZO-DCM** reduced by bioreductase

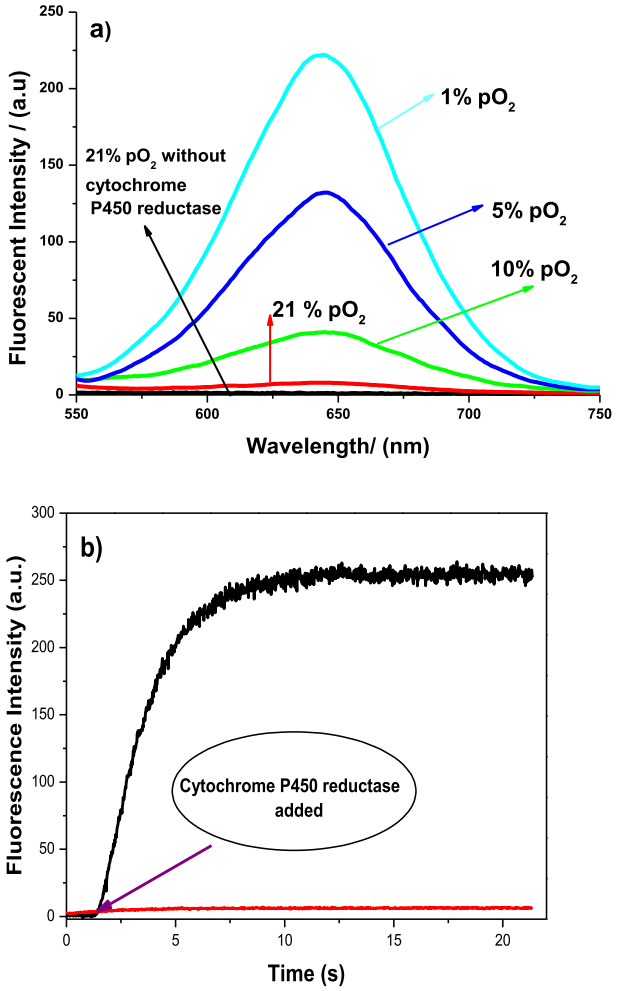

Fig. 2. a) Fluorescent changes of **AZO-DCM** without (pink curve) or with (other curve) under various oxygen levels. The spectra were measured in phosphate buffer (pH 7.4 with 10% DMSO and 0.1% Tween 80, contained 1 mM NADPH) at 37 °C; b) Time-dependent fluorescent intensity changes of **AZO-DCM** to cytochrome P450 reductase. The black curve means fluorescent intensity changes of **AZO-DCM** in the presence of cytochrome P450 and NADPH under hypoxia. The red curve means fluorescent intensity changes of **AZO-DCM** in the presence of cytochrome P450 and NADPH under normoxia condition. The fluorescence spectra were measured with excitation at 500 nm and the concentration of cytochrome P450 reductase is 1 U/mL. (For interpretation of the references to colour in this figure legend, the reader is referred to the web version of this article.)

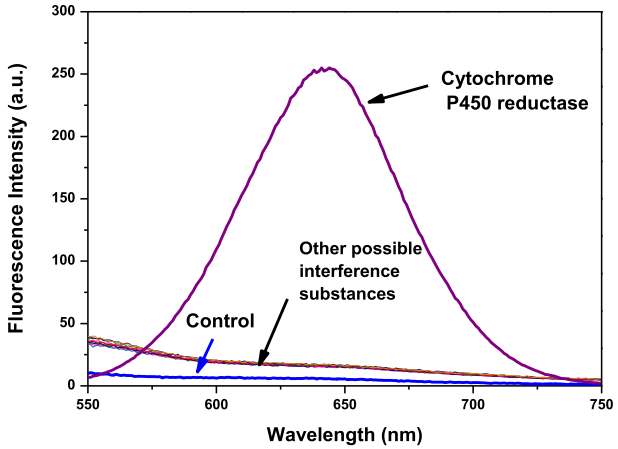

Fig. 3. Fluorescence response assays with the reductants. Control: probe **AZO-DCM** (3 μM). Fluorescence responses of **AZO-DCM** (3 μM) co-incubated with various reductants (1 mM) in PBS at room temperature with excitation wavelength at 500 nm. The reductants included Vc, glutathione, cysteine, dithiothreitol, $FeCl_2$, glucose, NADPH and tyrosine.

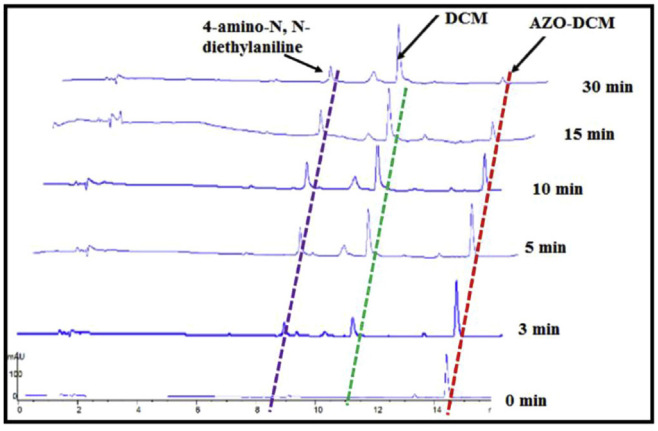

Fig. 4. HPLC analysis of metabolism of **AZO-DCM** reacted with cytochrome P450 reductase at different reaction time (0, 3, 5, 10, 15 and 30 min). **AZO-DCM** (3 μM) and NADPH (1 mM) was treated with cytochrome P450 reductase. HPLC profiles were detected by UV at 254 nm.

was confirmed by HPLC. Before the test, the retention time of the probe **AZO-DCM** and fluorophore **DCM** were determined. With the passage of reaction time, the concentration of **AZO-DCM** (the retention time was 14.4 min) decreased obviously, and it was almost disappeared after about 30 min (Fig. 4). Meanwhile, the concentration of fluorophore **DCM** (the retention time was 11.2 min) was increased gradually and obtained the maximum value after reacted 60 min. A peak in 8.7 min was another metabolism product 4-amino-N, *N*-diethylaniline, which also increased in about 30 min but decreased in the next 30 min. It maybe the substance was oxidized in the workup process. The HPLC also showed the azo bond was cleaved to two metabolism products by bioreductase with NADPH under hypoxia condition (Scheme 1).

3.7. Hypoxic cell imaging

For evaluation of the probe **AZO-DCM** applied in detecting the hypoxic condition in cancer cells, A549 cell lines were chosen for cellular fluorescent imaging. The A549 cells were incubated for 6 h under different oxygen concentration (pO_2 21%, 10%, 5% and 1%) which means different hypoxia state. As shown in Fig. 5, under normoxic condition (pO_2 is 21%), the fluorescent intensity was very weak. With the oxygen content decreased (from 10% to 1%), the fluorescent intensity was increased gradually. It was found that **AZO-DCM** had good selectivity to the pO_2. Using *Image J*™ software (1.47v), we calculated the average fluorescent intensity value at different oxygen condition (Fig. 5m). The mean fluorescent intensity increased from 0.066 to 10.08, nearly about 152-fold. HeLa cells were also applied in hypoxia detection and got the similar results (Fig. S1). These results indicated that the probe **AZO-DCM** could detect hypoxia cells sensitively. The outstanding performance was mainly because the fluorescent of **AZO-DCM** was totally quenched by azo bond.

4. Conclusion

In summary, we developed a novel fluorescent probe **AZO-DCM** by conjugating NIR fluorophore **DCM** with N, *N*-dimethylaniline through azo bond. In the present of NADPH, the probe performanced high selectivity to cytochrome P450 reductase over other bioreductants under hypoxia. The probe **AZO-DCM** could distinguish hypoxia cells with normoxic cells rapidly and sensitively. The fluorescent intensity was about 150-fold between hypoxia and

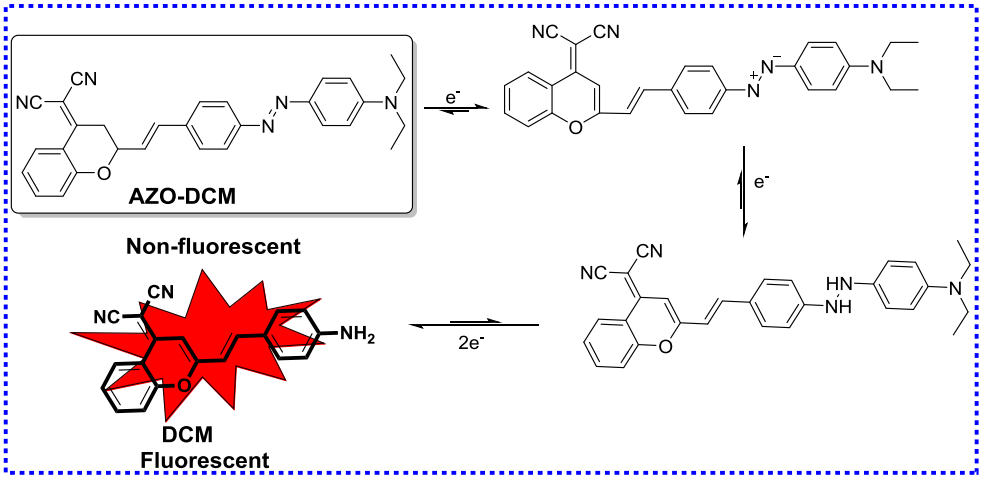

Scheme 1. The proposed mechanism of probe **AZO-DCM** reduced by Cytochrome P450 reductase and NADPH.

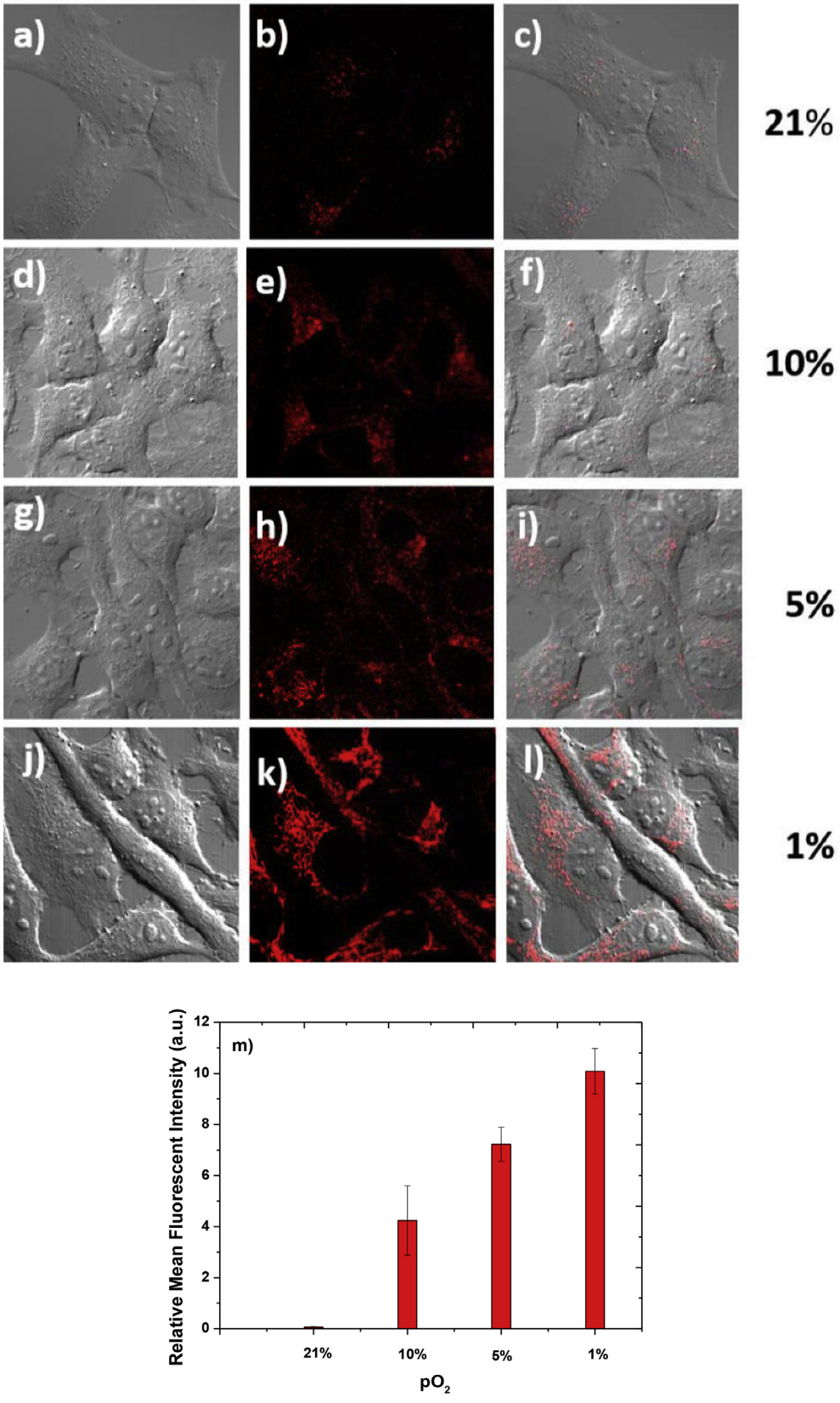

Fig. 5. Fluorescence microphotographs of A549 cells incubated with 1.0 μM fluorescent probe **AZO-DCM** at 37 °C. The first row was taken at aerobic condition (a, b and c). From the second row to the fourth row was taken at different hypoxic condition (10%, 5% and 1% pO_2), respectively. (a) (d) (g) and (j) were taken in bright field; (b) (e) (h) and (k) were taken in fluorescent model (red), (c) (f) (i) and (l) were the overlap of related bright field and fluorescent field. (m) The mean fluorescent photons and relative ratio. *Image J* software gave an average emission value of fluorescent photos. (For interpretation of the references to colour in this figure legend, the reader is referred to the web version of this article.)

normoxia condition, which indicated that **AZO-DCM** could be a candidate for hypoxia imaging.

Acknowledgments

We thank the National Natural Science Foundation of China (21602181, 21603143 and 31570360) for financial support. This work was also sponsored by the Shanghai leading talent project (3715341001) and Fundamental Research Funds for the Central Universities (XDJK2016C178).

Appendix A. Supplementary data

Supplementary data related to this article can be found at http://dx.doi.org/10.1016/j.dyepig.2016.12.062.

References

[1] Wilson WR, Hay MP. Targeting hypoxia in cancer therapy. Nat Rev Cancer 2011;11(6):393–410.
[2] Rockwell S, Dobrucki IT, Kim EY, Marrison ST, Vu VT. Hypoxia and radiation therapy: past history, ongoing research, and future promise. Curr Mol Med 2009;9(4):442–58.
[3] Traynor S, Gilham C, Foley R, Fairbairn LJ, Southgate TD, Worthington J, et al. Utilising a hypoxia-inducible suicide gene therapy strategy in combination with radiation to target prostate cancer cells. Radiother Oncol 2006;81. 477–477.
[4] Loughlin KR. Hypoxia inducible factor (HIF): its central role in renal cell cancer targeted therapy. Urol Oncol-Semin Ori 2009;27(3):236–7.
[5] Martin DS, Grocott MP. Oxygen therapy in critical illness: precise control of arterial oxygenation and permissive hypoxemia. Crit Care Med 2013;41(2): 423–32.
[6] Koh WJ, Rasey JS, Evans ML, Grierson JR, Lewellen TK, Graham MM, et al. Imaging of hypoxia in human tumors with [F-18] fluoromisonidazole. Int J Radiat Oncol Biol Phys 1992;22(1):199–212.
[7] Koch CJ, Jenkins WT, Jenkins KW, Yang XY, Shuman AL, Pickup S, et al. Mechanisms of blood flow and hypoxia production in rat 9L-epigastric tumors. Tumor Microenviron Ther 2013;1:1–13.
[8] Egeland TA, Gulliksrud K, Gaustad JV, Mathiesen B, Rofstad EK. Dynamic contrast-enhanced-MRI of tumor hypoxia. Magn Reson Med 2012;67(2): 519–30.
[9] Lee CT, Boss MK, Dewhirst MW. Imaging tumor hypoxia to advance radiation oncology. Antioxid Redox Signal 2014;21(2):313–37.
[10] Ammirante M, Shalapour S, Kang Y, Jamieson CA, Karin M. Tissue injury and hypoxia promote malignant progression of prostate cancer by inducing CXCL13 expression in tumor myofibroblasts. Proc Natl Acad Sci USA 2014;111(41):14776–81.
[11] Hockel M, Schlenger K, Aral B, Mitze M, Schaffer U, Vaupel P. Association between tumor hypoxia and malignant progression in advanced cancer of the uterine cervix. Cancer Res 1996;56(19):4509–15.
[12] Osinsky S, Zavelevich M, Vaupel P. Tumor hypoxia and malignant progression. Exp Oncol 2009;31(2):80–6.
[13] Lv J, Wang F, Qiang J, Ren X, Chen Y, Zhang Z, et al. Enhanced response speed and selectivity of fluorescein-based H_2S probe via the cleavage of nitrobenzene sulfonyl ester assisted by ortho aldehyde groups. Biosens Bioelectron 2016;87:96–100.
[14] Huang C, Jia T, Yu C, Zhang A, Jia N. An ESIPT based fluorescent probe for highly selective and ratiometric detection of periodate. Biosens Bioelectron 2015;63:513–8.
[15] Ma H, Zhou J, Shi W, Li L, Gong Q, Wu X, et al. A lysosome-targeting fluorescence off-on probe for imaging of nitroreductase and hypoxia in live cells. Chem Asian J 2016;11(16):2719–24.
[16] Zhang J, Liu HW, Hu XX, Li J, Liang LH, Zhang XB, et al. Efficient two-photon fluorescent probe for nitroreductase detection and hypoxia imaging in tumor cells and tissues. Anal Chem 2015;87(23):11832–9.
[17] Wan QQ, Gao XH, He XY, Chen SM, Song YC, Gong QY, et al. A cresyl violet-based fluorescent off-on probe for the detection and imaging of hypoxia and nitroreductase in living organisms. Chem Asian J 2014;9(8):2058–62.
[18] Guo T, Cui L, Shen J, Zhu W, Xu Y, Qian X. A highly sensitive long-wavelength fluorescence probe for nitroreductase and hypoxia: selective detection and quantification. Chem Comm 2013;49(92):10820–2.
[19] Cui L, Zhong Y, Zhu W, Xu Y, Du Q, Wang X, et al. A new prodrug-derived ratiometric fluorescent probe for hypoxia: high selectivity of nitroreductase and imaging in tumor cell. Org Lett 2011;13(5):928–31.
[20] Kiyose K, Hanaoka K, Oushiki D, Nakamura T, Kajimura M, Suematsu M, et al. Hypoxia-Sensitive fluorescent probes for in vivo real-time fluorescence imaging of acute ischemia. J Am Chem Soc 2010;132(45):15846–8.
[21] Piao W, Tsuda S, Tanaka Y, Maeda S, Liu F, Takahashi S, et al. Development of azo-based fluorescent probes to detect different levels of hypoxia. Angew Chem Int Ed Engl 2013;52(49):13028–32.
[22] Cai Q, Yu T, Zhu W, Xu Y, Qian X. A turn-on fluorescent probe for tumor hypoxia imaging in living cells. Chem Comm 2015;51(79):14739–41.
[23] Gu K, Liu Y, Guo Z, Lian C, Yan C, Shi P, et al. In situ ratiometric quantitative tracing of intracellular leucine aminopeptidase activity via an activatable near-infrared fluorescent probe. ACS Appl Mater Interfaces 2016;8(40): 26622–9.
[24] Wu X, Sun X, Guo Z, Tang J, Shen Y, James TD, et al. In vivo and in situ tracking cancer chemotherapy by highly photostable NIR fluorescent theranostic prodrug. J Am Chem Soc 2014;136(9):3579–88.
[25] Li GY, Chen Y, Wang JQ, Lin Q, Zhao J, Ji LN, et al. A dinuclear iridium(III) complex as a visual specific phosphorescent probe for endogenous sulphite and bisulphite in living cells. Chem Sci 2013;4(12):4426–33.
[26] Tan L, Lin W, Zhu S, Yuan L, Zheng K. A coumarin-quinolinium-based fluorescent probe for ratiometric sensing of sulfite in living cells. Org Biomol Chem 2014;12(26):4637–43.
[27] Tian H, Qian J, Sun Q, Bai H, Zhang W. Colorimetric and ratiometric fluorescent detection of sulfite in water via cationic surfactant-promoted addition of sulfite to alpha,beta-unsaturated ketone. Anal Chim Acta 2013;788:165–70.
[28] Li GY, Liu JP, Huang HY, Wen Y, Chao H, Ji LN. Colorimetric and luminescent dual-signaling responsive probing of thiols by a ruthenium(II)-azo complex. J Inorg Biochem 2013;121:108–13.
[29] Li G, Chen Y, Wu J, Ji L, Chao H. Thiol-specific phosphorescent imaging in living cells with an azobis(2,2[prime or minute]-bipyridine)-bridged dinuclear iridium(iii) complex. Chem Comm 2013;49(20):2040–2.
[30] Joe O, Kinu S, Masayuki T, Naotoshi O, Koji A, Manabu S. Ruthenium complexes containing an azobipyridine ligand as redox-responsive molecular switches. Chem Lett 1996;25(10):847–8.